Doping of GaN with Mg: factors limiting hole concentration

© I.Yu. Evstratov, S.Yu. Karpov

Soft-Impact Ltd.,
194044 St. Petersburg, Russia

E-mail: sergey.karpov@softimpact.ru

On the basis of published well-performed temperature-dependent Hall measurements (TDHMs) their conventional processing procedure and information to be obtained is reconsidered. We discuss a temperature range suitable for accurate data treatment, the use of proper materials properties for data approximation, and two-carrier model application to account for impurity-band hole conduction in GaN:Mg. Improved processing procedure enables separate estimating concentrations of free and acceptor-bound holes, determining concentration-dependent acceptor ionization energy, and finding a correlation between compensating donors and acceptors concentrations. On the basis of the correlation found and additional experimental data, a new mechanism of Mg acceptor self-compensation is suggested, involving formation of $Mg_{Ga}-H_N$ defect complexes. Analysis of impurity-band conductivity has revealed its hopping mechanism.

Keywords:cGaN, p-type doping, Hall measurements, acceptor ionization energy, impurity-band conduction, hopping conductivity, self-compensation of Mg acceptors.

DOI: 10.61011/SC.2026.04.64079.9611

1. Introduction

Magnesium is the only impurity providing in GaN the room-temperature (RT) hole concentration acceptable for various device applications. There are two main factors limiting the hole concentration. One is a high acceptor ionization energy (AIE). The experimental low-concentration AIE determined by photoluminescence (PL) ranges from 215 to 245 meV with the mean value of about 226 meV [1–5]. A similar scatter in the AIE values, from 204 to 253 meV, has been obtained theoretically by using the $\mathbf{k}\cdot\mathbf{p}$ Hamiltonian combined with artificially adjusted potential energy of the Mg impurity [6,7]. The scatter largely originated from differences in the parameters of the $\mathbf{k}\cdot\mathbf{p}$ Hamiltonian borrowed from various sources. *Ab initio* calculations predict the ionization energy to be of 223 meV [5] 230 meV [8], 260 meV [9], and 326 meV [10]. So, the uncertainty in the low-concentration ionization energy still remains too high from both experimental and theoretical points of view.

Increasing Mg concentration in GaN results in substantial AIE reduction. The thermal AIEs of 150−190 meV were observed when the concentration of Mg acceptors increased from $1\cdot10^{19}$ to $8\cdot10^{19}\,cm^{-3}$ (see experimental points in Figure 7, *b*) and its further reduction down to 50−60 meV was reported in [11]. No reliable data on achieving the Mott transition in the heavily doped GaN:Mg has been reported to date in spite of the practical interest to low-temperature operation of blue and green light-emitting diodes [12–14]. A principal reason for this is self-compensation of the Mg acceptors at high concentrations, which is the second factor limiting the RT hole conductivity.

The self-compensation implies massive generation of donor-type defects, starting at a certain high Mg concentration in GaN and leading to a threshold-like drop of the hole concentration at RT. One can characterize the onset of self-compensation with two parameters: the maximum hole concentration p_{max} achieved, for instance, at RT and the Mg concentration N_{max} corresponding to p_{max}. It turned out the both parameters to be noticeably dependent on *p*-GaN growth conditions and particular growth technique — see Table 1. In the most of cases considered in Table 1, growth of *p*-GaN by Metal-Organic Vapor Phase Epitaxy (MOVPE) was followed by a sample annealing in nitrogen atmosphere typically at 550−750 °C with the aim to release interstitial hydrogen accumulated inside the semiconductor during the growth and being able to passivate the Mg acceptors. In the case of *p*-GaN growth by Plasma-Assisted Molecular Beam Epitaxy (PAMBE) or pulsed sputtering deposition the annealing procedure was not be necessary to apply due to the absence of hydrogen atmosphere during growth.

The dependence of self-compensation onset on the *p*-GaN growth conditions implies involvement of point defects other than Mg acceptors on Ga-sites (Mg_{Ga}) and being donors capable of compensating the Mg acceptors. Various defects have been considered as the compensating donors: nitrogen vacancy (V_N) being a triple donor and $Mg_{Ga}-V_N$ complex being a double donor [15,18], Mg interstitial (Mg_I) being double donor [24], V_N-H_I complex (double donor in *p*-type GaN) [25], and $V_N-(V_{Ga})_s$ ($s=2-3$) complexes. The latter ones have been suggested in the study of GaN implanted with Mg and annealed at temperatures 1000−1300 °C [26]. However, no reliable way to identify the most probable candidate for principal compensating donors has been found up to date.

Since increasing the hole concentration in GaN:Mg requires either to shift N_{max} towards higher Mg concentrations (Table 1 demonstrates that it is feasible) or/and to reduce AIE of the acceptors as far, as possible, better understanding of factors affecting and limiting the both parameters is necessary. A conventional technique suitable for this is the TDHMs of the hole concentration and mobility. There are many studies in literature using this technique and providing

Table 1. Maximum RT hole concentrations p_{max} and corresponding Mg concentrations N_{max} in p-GaN grown by various techniques. Growth temperature T_g of p-GaN layer is also provided, if available

Growth technique	T_g (°C)	p_{max}, cm^{-3}	N_{max}, cm^{-3}	Ref.
MOVPE of (0001)GaN on sapphire	1025	$6 \cdot 10^{17}$	$2 \cdot 10^{19}$	[15]
PAMBE of (0001)GaN on sapphire	650	$1.4 \cdot 10^{18}$	$8 \cdot 10^{19}$	[16]
MOVPE of (0001)GaN on sapphire		$9 \cdot 10^{17}$	$3 \cdot 10^{19}$	[17]
MOVPE of (0001)GaN on sapphire		$1.2 \cdot 10^{18}$	$8-10 \cdot 10^{19}$	[18]
MOVPE of $(10\bar{1}\bar{1})$GaN on $MgAl_2O_4$		$2.4 \cdot 10^{18}$	$3.3 \cdot 10^{19}$	[19]
MOVPE of (0001)GaN on sapphire	1020	$4 \cdot 10^{17}$	$3 \cdot 10^{19}$	[20]
MOVPE 0f (0001)GaN on (111)Si	990	$8.7 \cdot 10^{17}$	$6 \cdot 10^{19}$	[21]
MOVPE on free-standing (0001)GaN	960	$1.3 \cdot 10^{18}$	$4 \cdot 10^{19}$	[22]
Pulsed sputtering deposition on bulk GaN	550−650	$6 \cdot 10^{18}$	$2 \cdot 10^{20}$	[23]

the detailed data on the hole concentrations at various Mg concentrations in GaN. Unfortunately, interpretation of the data suffers from uncertainty in the specific values of materials parameters relevant to determination of AIE, like effective masses of holes necessary for calculating the density of hole states, hole degeneracy factor, etc. As a rule, the complex valence band structure of GaN is also ignored in the analysis of the Hall data despite the fact that both crystal-field and spin-orbital splitting energies in GaN are comparable with the thermal energy at RT. All this introduces a noticeable inaccuracy into the hole parameters extracted from TDHMs. And, as it will be shown in Sec. 2.3, the impurity-band hole conduction should be accounted for in the analysis of the Hall data at high Mg concentrations because this factor may also interfere the extracted parameters.

The purpose of the paper is to apply the improved processing procedure to the Hall data available in literature in order to get a deeper insight into the factors determining the AIE and the onset of Mg acceptor self-compensation in GaN. After careful choice of the GaN band-structure parameters necessary for accurate processing of the TDHM data, AIE and concentration of compensating donors N_D is derived in a wide range of the Mg concentrations N_A. The dependence of N_D on N_A extracted from the Hall data enables making a guess on the nature of compensating donors and mechanism of Mg acceptor self-compensation.

The paper is organized as follows. Section 2 presents the theoretical background underlying an accurate interpretation of the temperature-dependent Hall data and proper GaN band structure parameters necessary for this purpose. Application of the improved procedure of the Hall data processing to a number of well-performed experiments and the results of the processing are discussed in Section 3. Section 4 summarizes this study and gives the most important conclusions.

2. Theoretical background

Here, the theoretical background necessary for correct interpretation of the Hall data is described and the choice of the most reliable GaN band structure parameters is made for accurate processing of the Hall data.

2.1. Acceptor states and degeneracy factor

According to [27], the degeneration degree of the acceptor ground state in wurtzite crystals is similar to that of the valence band in the Γ-point of the Brillouin zone. In the absence of the crystal-field and spin-orbital splitting, this would correspond to a sixfold degenerated acceptor state. The crystal field and spin-orbital interaction split the acceptor ground state into three twofold-degenerated sublevels, marked hereafter by letters A, B, and C, with the mutual energy separation much smaller than the acceptor activation energy by itself. In this case, the ionized acceptor concentration N_A^- depends on the total acceptor concentration N_A as follows:

$$N_A^- = N_A \left\{ 1 + \sum_{i=A,B,C} g_i \exp\left[(E_V + E_i - F)/kT\right] \right\}^{-1}, \quad (1)$$

where $g_i = 2$ is the degeneracy factor of the i-th acceptor sublevel ($i = A, B, C$), E_i is the ionization energy corresponding to the i-th acceptor sublevel, F is the Fermi level, k is the Boltzmann constant, and T is temperature. The parameter $E_V = \max_s\{E_s\}$ is the energy position of the valence band top, where E_s corresponds to the top of the s-th hole subband, i.e. that of heavy holes ($s = hh$), light holes ($s = lh$), or split-off holes ($s = sh$). The energy separations between the heavy-hole subband and those of light (Δ_{hl}) and split-off (Δ_{hs}) holes can be determined within the $\mathbf{k} \cdot \mathbf{p}$ model [28] developed for wurtzite semiconductors:

$$\Delta_{hl} = \frac{1}{2}\left(\Delta_{cf} + \Delta_{so} - \sqrt{(\Delta_{cf} + \Delta_{so})^2 - \frac{8}{3}\Delta_{cf}\Delta_{so}} \right), \quad (2a)$$

$$\Delta_{hs} = \frac{1}{2}\left(\Delta_{cf} + \Delta_{so} + \sqrt{(\Delta_{cf} + \Delta_{so})^2 - \frac{8}{3}\Delta_{cf}\Delta_{so}} \right). \quad (2b)$$

Here Δ_{cf} is the crystal-field splitting and Δ_{so} is the spin-orbital splitting of the valence band. With the band-structure

Table 2. Band structure and other parameters of GaN used in this study

Parameters	Low-k values	High-k values	Ref.
Crystal-field splitting of the valence band, meV	10		[30]
Spin-orbital splitting of the valence band, meV	18		[30]
Longitudinal heavy hole effective mass, m^z_{hh}/m^*_0	1.876	1.876	[31]
Transverse heavy hole effective mass, m^t_{hh}/m_0	0.329	1.887	[31]
Longitudinal light hole effective mass, m^z_{lh}/m_0	1.081	1.876	[31]
Transverse light hole effective mass, m^t_{lh}/m_0	0.350	0.180	[31]
Longitudinal split-off hole effective mass, m^z_{sh}/m_0	0.180	0.168	[31]
Transverse split-off hole effective mass, m^t_{sh}/m_0	1.409	1.894	[31]
Longitudinal static dielectric constant, κ_z	10.4		[32]
Transverse static dielectric constant, κ_t	9.5		[32]

* m_0 in the table is the electron mass in vacuum.

parameters listed in Table 2, the separations of the valence subbands are: $\Delta_{hl} = 5.3\,\text{meV}$ and $\Delta_{hs} = 22.7\,\text{meV}$ (the separation between the subbands of light and split-off holes $\Delta_{ls} = \Delta_{hs} - \Delta_{hl} = 17.4\,\text{meV}$).

Theoretical estimations of the acceptor ground state splitting in *p*-GaN were made in [29] by using a Luttinger's Hamiltonian in the spherical approximation. It has been shown that the energy separations $\Delta_{AB} = E_A - E_B$ and $\Delta_{AC} = E_A - E_C$ between the acceptor ground state sublevels could be found from Eqs. (2) with renormalized crystal-field ($\Delta^*_{cf} = x_{cf}\Delta_{cf}$) and spin-orbital ($\Delta^*_{so} = x_{so}\Delta_{so}$) splittings used instead of the valence-band ones. The dimensionless renormalization coefficients x_{cf} and x_{so} were found to depend on the ratio of the light to heavy hole effective masses $\beta = m_{lh}/m_{hh}$. The values $x_{cf} = 0.8$ and $x_{so} = 0.67$ (at $\beta = 0.127$) were derived in [29] for GaN from the longitudinal ($m^z_{hh} = 2.03m_0$) and transverse ($m^t_{hh} = 0.33m_0$) effective masses of heavy holes (m_0 is the free electron mass), using a special procedure. The corresponding ionization energy of a single acceptor (or, the same, the low-concentration AIE) $E^0_A = 205\,\text{meV}$ was then estimated in [29] by zero-range potential model, assuming an effective static dielectric constant to be of 9.5.

It should be noted that such a large anisotropy of the above heavy-hole effective masses, m^z_{hh} and m^t_{hh}, is a specific feature of their correspondence to small values of the hole wave vector **k** near the Γ-point of the Brillouin zone (see [28] for definition and derivation of the low-k and high-k effective masses). The use of alternative low-k masses listed in Table 2 provides, for example: $\beta = 0.138$, $x_{cf} = 0.81$, $x_{so} = 0.68$, and $E^0_A = 174\,\text{meV}$ with the procedure of m_{lh} and m_{hh} determination suggested in [29] and the static dielectric constant $\kappa = (\kappa_z\kappa_t)^{1/2}$ evaluated from the longitudinal κ_z and transverse κ_t dielectric constants given in Table 2. However, the Bohr radius corresponding to the above values of E^0_A is rather small, so that large **k**-vectors contribute definitely into the wave function of a hole bound by an acceptor. Therefore, high-k effective masses should be used for evaluation of the renormalization coefficients x_{cf} and x_{so}. The use of the high-k masses from Table 2 provides $\beta \approx 1$ and, therefore, $x_{cf} = x_{so} \approx 1$. Thereby, one obtains $\Delta_{AB} \approx \Delta_{hl}$ and $\Delta_{AC} \approx \Delta_{hs}$ to be used for determining the acceptor level splittings by Eq. (2). And, with the high-k masses of heavy holes taken from Table 2, the ionization energy of a single acceptor $E^0_A = 257\,\text{meV}$, which slightly exceeds the values typically obtained by PL measurements [1–5].

Thus, the upper acceptor levels in GaN should include two sublevels, *A* and *B*, close to each other, and a sublevel *C* well separated from *A* and *B*. This picture is consistent with the observation of two distinct acceptor levels in *p*-GaN made by transient admittance spectroscopy [33]. The level having the ionization energy of 160 meV measured in [33] may be associated with the sublevels *A* and *B* that could not be resolved experimentally because of their small separation. The level with the measured ionization energy of 135 meV can be, in turn, associated with the sublevel *C*. The energy difference of 25 meV between the two ionization energies is close to the acceptor level splitting $\Delta_{AC} \approx \Delta_{hs} = 22.7\,\text{meV}$ estimated above. Similar results have been obtained earlier in [34]. In that study, two levels with ionization energies of 160 and 124 meV were registered by admittance spectroscopy in a sample with a lower Mg concentration, while the only level with the ionization energy of 136 meV was found in a sample with a higher doping. The difference between the ionization energies is 36 meV in this case, corresponding, however, to different samples. Two deep levels apparently related to Mg acceptor with the ionization energies of 170 and 130 meV were also reported in [35].

With account of the ground acceptor state splitting by the crystal field and spin-orbital interaction, the expression (1) can be transformed in a more convenient form:

$$N^-_A = \frac{N_A}{1 + \tilde{g}_A \exp[(E_V + E_A - F)/kT])}, \qquad (3)$$

where

$$\tilde{g}_A = 2[1 + \exp(-\Delta_{AB}/kT) + \exp(-\Delta_{AC}/kT)] \qquad (4)$$

is the temperature-dependent effective degeneracy factor, and the ionization energy E_A is associated with the deepest acceptor sublevel *A*. A similar procedure for $\tilde{g}_A$ evaluation

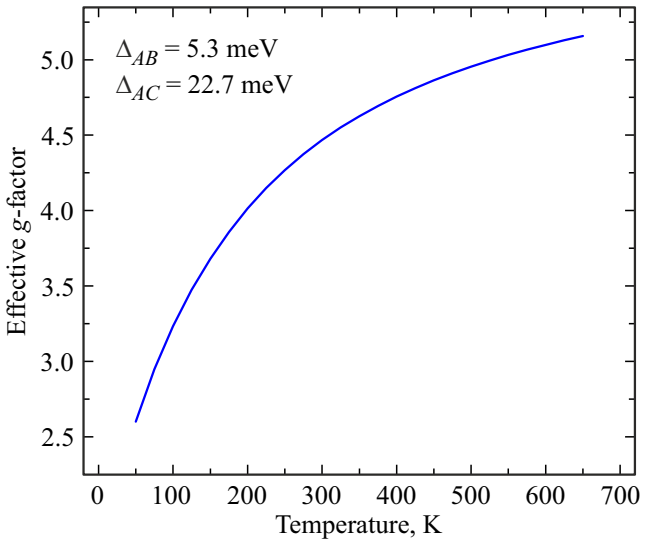


Figure 1. Temperature dependence of the effective degeneracy factor $\tilde{g}_A$ of acceptor states calculated with $\Delta_{AB} = 5.3$ meV and $\Delta_{AC} = 22.7$ meV.

was suggested earlier in [15]. The temperature dependence of the effective degeneration factor $\tilde{g}_A$ of the acceptor level in GaN is plotted in Figure 1. One can see that $\tilde{g}_A$ varies from 2.60 to 4.95, if the temperature rises from 50 to 500 K and is equal to 4.47 at RT. So, the values of $\tilde{g}_A$ differ remarkably from the values of 2 [36,37] or 4 [11,17,37,39] frequently used for AIE extraction from the Hall data. In other words, this temperature dependence is essential and should be accounted for while processing TDHM data.

2.2. Hole effective masses and free carrier concentration in *p*-GaN

The concentration of free holes p can be calculated assuming the case of non-degenerate semiconductor and accounting for the complex valence band structure of GaN

$$p = \sum_{s=hh,lh,sh} N_s \exp\left(\frac{E_s - F}{kT}\right) = \exp\left(\frac{E_V - F}{kT}\right) \sum_{s=hh,lh,sh} N_s \exp\left(\frac{E_s - E_V}{kT}\right). \quad (5)$$

Here $N_s = 2m_s^t (m_s^z)^{1/2} (kT/2\pi\hbar^2)^{3/2}$ is the density of states in the respective hole subband, m_s^t and m_s^z are the transverse and longitudinal hole effective masses in the s-th subband, respectively, and $\hbar$ is the reduced Plank constant.

The Fermi level F can be found from the electrical neutrality condition in the bulk of the p-GaN semiconductor: $N_A^- = p + N_D$ where N_D is the total residual/compensating donor concentration assumed to be equal to the ionized donor concentration in p-GaN. Combining Eqs. (3)–(5) one can obtain

$$N_A N_V / (N_V + g_A^* p) = p + N_D, \quad (6)$$

where the parameter $g_A^* = \tilde{g}_A \exp(E_A/kT)$ and $N_V = \sum_{s=hh,lh,sh} N_S \exp[(E_s - E_V)/kT]$ is the effective density of hole states.

The equation (6) allows the analytical solution

$$p = \frac{[\sqrt{(N_V + g_A^* N_D)^2 + 4 g_A^* N_V (N_A - N_D)} - (N_V + g_A^* N_D)]}{2 g_A^*}. \quad (7)$$

Qualitative analysis of Eq. (7) shows the variation of the hole concentration with temperature to depend significantly on the concentration of residual/compensating donors N_D, which is a direct consequence of high ionization energy of the Mg acceptors. Indeed, at $E_A \gg kT$ the factor g_A^* may be very high, modifying the temperature dependence of the hole concentration even if $N_D \ll N_A$. In particular, with the typical value $E_A = 170$ meV, the factor g_A^* is equal to $3.7 \cdot 10^8$ at the temperature of 100 K and to $1.4 \cdot 10^2$ at the temperature of 400 K, i. e. it changes by more than six orders of magnitude. This circumstance marks out GaN from conventional III-V semiconductors having much lower AIEs.

With account of the above remark, three different sections can be normally distinguished in the temperature dependence of hole concentration (see Figure 2). Section I corresponds to a very high temperature at which $N_V \gg g_A^* N_A$ and $N_A > N_D$. Here $p \cong N_A$, as follows from Eq. (7), i. e. the hole concentration is limited by the total acceptor concentration and does not depend on temperature. At a somewhat lower temperature, where $g_A^* N_D \ll N_V \ll g_A^* N_A$, the hole concentration $p \cong (N_A N_V / g_A^*)^{1/2}$. Such a condition corresponds to section II, and the slope of the temperature dependence is roughly equal to $E_A/2$ (to get this estimate, the power-like temperature dependence of the density of states N_V is neglected). Finally, at much lower temperature, when the effective density of states $N_V \ll g_A^* N_D$, the hole concentration $p \cong N_V (N_A/N_D - 1)/g_A^*$. This is the case of section III where the slope of the dependence of hole concentration upon inverse temperature is nearly equal to E_A, if the variation of density of states with temperature is again neglected.

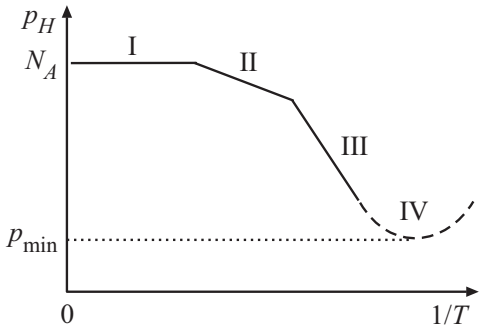


Figure 2. Schematic variation of the apparent hole concentration p_H obtained by TDHMs with the inverse temperature $1/T$ where specific sections exhibiting different slopes are shown. See text for more detail.

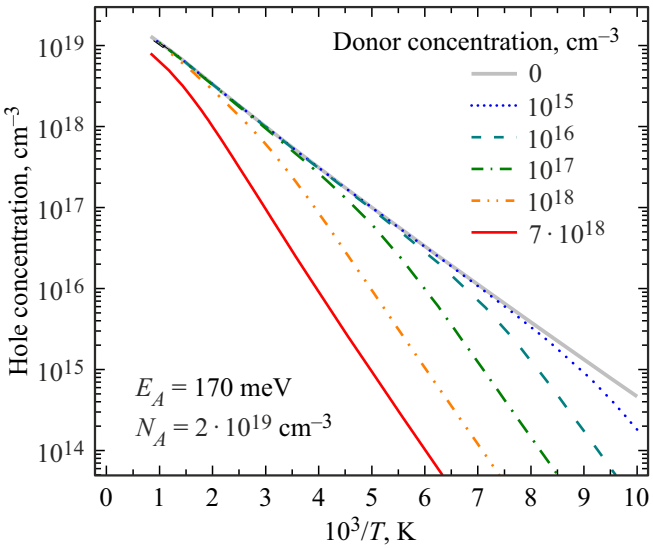


Figure 3. Free hole concentration as a function of inverse temperature calculated at the constant acceptor concentration of $2 \cdot 10^{19}$ cm^{-3} and various residual donor concentrations. AIE of 170 meV is assumed in the calculations.

The above analysis shows that only section III enables direct estimation of AIE from the slope of the hole concentration dependence on inverse temperature. In practice, however, high temperatures corresponding to section I cannot be reached. Besides, the region of impurity-band conduction (section IV) frequently appears at relatively low temperatures, as shown schematically by dashed line in Figure 2. This region spreads considerably with increasing doping level in the material. At a very high p-doping, section IV may expand up to the end of section II, gobbling up completely section III. Here, no reliable estimation of AIE becomes possible from the slope of the temperature-dependent hole concentration.

One more feature of GaN and other III-nitride semiconductors is that typical acceptor concentration N_A is normally comparable with the density of states N_V. This results in the fact that the temperature dependence of the hole concentration in a high-quality material, i.e. that having negligibly small donor concentration N_D, behaves like in section II in Figure 2. In this case, the directly measured slope of the dependence does not correspond again to the actual AIE.

To illustrate the above remark, Figure 3 plots the free hole concentration versus 1000/T calculated by Eq. (7) at various residual donor concentrations but with the same concentration of acceptors and their ionization energy. One can see from the figure that the slopes of the calculated curves and absolute values of the hole concentrations are quite sensitive to the chosen N_D.

The above analysis demonstrates importance of choosing a proper temperature range for extraction of AIE from TDHM data. First, the use of a narrow temperature interval and determination of AIE by the slope of hole concentration dependence on $1/T$ may produce a large inaccuracy. So, the choice of a wide T-range, where the slope is generally varied, and fitting the TDHM data in the whole range enables considerable reduction of possible inaccuracy. Second, in order to diminish the data interference from the impurity-band hole conduction it is desirable to choose the temperature range near RT and well above it. In this case, one can be sure that the impurity-band impact on the TDHMs is negligible.

The next important point to be discussed is the choice of the hole effective masses to calculate the density of states N_V. According to [28], the hole effective masses vary rapidly with the wave vector **k** from the values corresponding to the Γ-point of the Brillouin zone (k = 0) to those related to energies well exceeding both the spin-orbital and crystal-field splittings. The two sets of the effective masses corresponding to either low-k or high k values are given in Table 2, providing the RT effective density of states N_V equal to $2.0 \cdot 10^{19}$ and $7.2 \cdot 10^{19}$ cm^{-3}, respectively. The contributions of various hole subbands to the total density of states N_V as a function of temperature calculated for low-k and high-k effective masses are plotted in Figure 4. One can see that the low-k masses provide the contributions of heavy, light, and split-off holes more or less comparable with each other. In contrast, a dominant contribution of the heavy holes is predicted in the case of high-k masses.

Generally, one could using the complex energy dispersion of every valence subband to calculate rigorously N_V. This would provide a gradual transition from the low-k effective masses to high-k ones while temperatures increasing. In this study we use, however, a simplified approach, employing the high-k effective masses only. Such a simplification will be justified below by a good agreement of the predicted temperature dependence of hole concentration with experimental data obtained in a wide range of temperature variation. With the above simplification, this study is close to Ref. [17] where an isotropic hole effective mass $m_{hh} = 2.2m_0$ has been used for calculating the total density of hole states.

2.3. Accounting for hole conduction via impurity band

As it was mentioned in the previous section, the hole conduction via impurity band may interfere substantially the hole-concentration, if the temperature is not so high. In order to account the impact of such a transport mechanism, a two-carrier model can be used, considering parallel transport of free holes in the valence band and holes bound by acceptors in the impurity band. According to the model, the apparent hole concentration p_H obtained by the Hall measurements is related to the concentration of free holes p in the valence band by the equation (see, for instance, [40]):

$$p_H = \frac{(p + \gamma N_A^0)^2}{p + \gamma^2 N_A^0}, \quad \gamma = \frac{\mu_h}{\mu_p}, \quad N_A^0 = N_A - N_D - p. \quad (8)$$

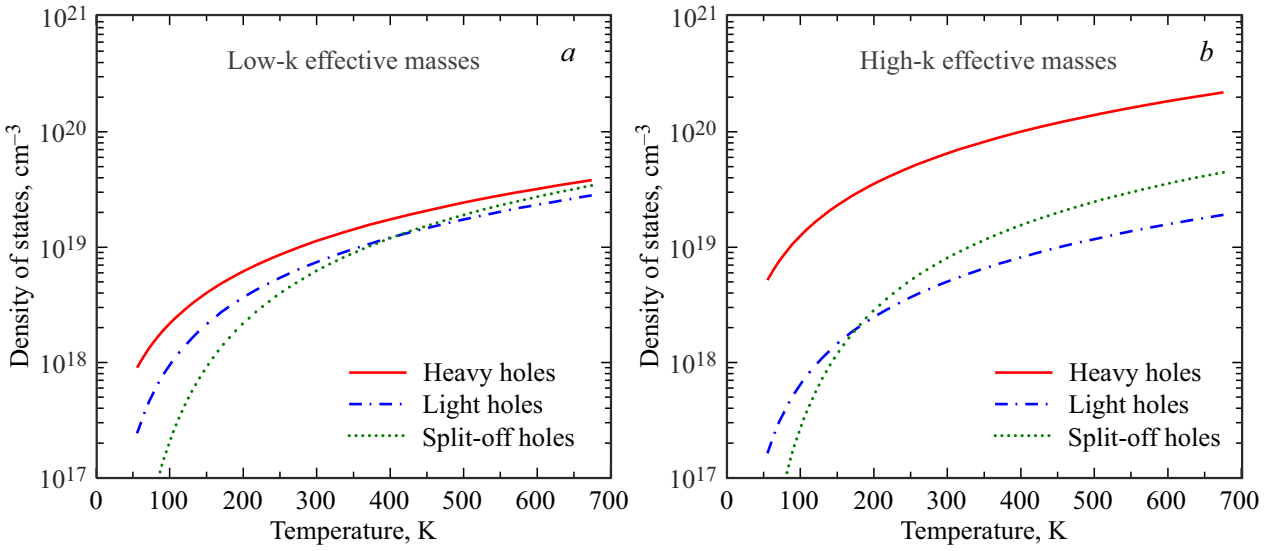


Figure 4. Contributions of heavy, light and split-off holes to the density of states N_V as a function of temperature calculated for low-k (a) and high-k (b) sets of effective masses.

Here μ_p is the mobility of free holes in the valence band, μ_h is the mobility of bound holes, and N_A^0 is the neutral acceptor concentration or, the same, the concentration of holes bound with the acceptors. Normally, the mobility ratio γ is many orders of magnitude less than unity and the apparent mobility obtained by Hall measurements is

$$\mu_H = \frac{(\mu_p p + \mu_h N_A^0)}{p_H} = \frac{\mu_p (p + \gamma^2 N_A^0)}{p + \gamma N_A^0}. \qquad (9)$$

At sufficiently high temperature, where $p \gg \gamma N_A^0$, the apparent hole concentration $p_H \cong p$, increasing with temperature, and the apparent hole mobility is $\mu_H \cong \mu_p$. At a relatively low temperature, where $\gamma^2 N_A^0 \ll p \ll \gamma N_A^0$, the apparent concentration $p_H \cong (\gamma N_A^0)^2/p$, decreasing with temperature, and the apparent hole mobility is $\mu_H \cong \mu_h (p/N_A^0)$. Transition from the low to high temperature occurs at a minimum of the apparent hole concentration $p_{\min}$ (see Figure 2), i. e. at the point corresponding to the relationship $p \cong \gamma N_A^0$. At this point, one can obtain: $p_H \cong 4\gamma N_A^0$ and $\mu_H = 2\mu_h N_A^0/p_H \cong \frac{1}{2}\mu_p$. The latter expression enables estimating the bound hole mobility μ_h from the experimental data on the apparent hole concentration and mobility at the point corresponding to $p_{\min}$.

The Hall factor r_H is conventionally defined as the ratio of p to p_H. Normally, extraction of free hole concentration from TDHM data is based on the assumption that $r_H = 1$. On the other hand, the expression for the Hall factor coming from Eq. (8) reads: $r_H = p(p + \gamma^2 N_A^0)/(p + \gamma N_A^0)^2 \cong (1 + \gamma N_A^0/p)^{-1}$. In particular, at p_H close to $p_{\min}$ the Hall factor $r_H \cong 0.5$. If γN_A^0 becomes greater than p at low temperatures, the Hall factor may be remarkably lower than unity. Therefore, disregarding the impurity-band hole conduction and choosing a relatively low-temperature range for TDHMs may result in remarkable overestimating the concentration of free holes.

3. Result and discussion

Very frequently processing of the TDHM data includes (i) simultaneous fitting the acceptor concentration N_A and the residual/compensating donor concentration N_D to approximate the experimental p_H dependence on the inverse temperature $1/T$, and then (ii) AIE determination from the slope of the $p_H(1/T)$ approximation curve. As it was shown in Sec. 2.2, such a procedure may produce a large inaccuracy. Even when AIE is alternatively included into the set of fitting parameters, the conventional processing procedure may result in ambiguous determination of the N_A, N_D, and E_A values, especially, if a narrow or improper range of temperatures is chosen for TDHMs.

To avoid such an ambiguity, well-performed TDHM data were selected from literature for analysis. First, all the selected data were obtained in rather wide temperature ranges, including both margins: well above and well below RT. Second, the data cover a large range of Mg acceptor concentrations, from $5 \cdot 10^{18}$ to $8 \cdot 10^{20}$ cm^{-3}. Third, most of the data were accompanied by independent estimation of the Mg atomic concentrations in GaN samples by SIMS. These concentrations were associated with N_A, so that only two parameters N_D and E_A, remain to be fitted to the selected data. In these cases, however, it was specially checked that alternative fitting of three parameters, N_A, N_D, and E_A, enabled very close results. Finally, the processing of the selected data was carried out by two-carrier model (see Sec. 2.3) with the mobility ratio γ regarded as one more temperature-independent fitting parameter. The latter enabled accounting effects of the

impurity-band hole conduction and crude estimating the mobility of holes bound on acceptors.

3.1. Accurate fitting of Hall data

We start our analysis with detailed data reported in [17] for heavy-doped p-GaN with the Mg concentration varied from $1.6 \cdot 10^{19}$ to $8 \cdot 10^{20}\,\mathrm{cm}^{-3}$. The results of the model parameter fitting are compared in Figure 5 with the TDHMs reported in [17]. First, one can see from the figure that two-carrier model used for fitting adequately reproduces the temperature dependence of the apparent hole concentration in a wide temperature range, including the regions of impurity-band conduction. Second, only samples A and B would allow distinguishing section III between sections II and IV in the plotted curves. In other samples, section III cannot be found at all because of sections II and IV overlapping. This means that the slope of the curves obtained for samples C–F does not correspond to real AIE. Third, rather low ionization energies, $\sim 100-110$ meV, have been obtained by fitting for samples D and E. The ionization energy reduction is accompanied by dramatic increase in the compensating donor concentration at increasing N_A, as shown in the legends to the plots in Figure 5. At high temperatures, the hole concentration in samples D and E becomes as high, as $\sim 5-7 \cdot 10^{19}\,\mathrm{cm}^{-3}$. The ionization energy is restored back to 140 meV in sample F where the donor concentration becomes comparable with the acceptor concentration determined by SIMS.

A similar fitting has been applied to the data of [37,41] (see Figure 6). Only the data for the sample $s4$ were borrowed from [37] as those demonstrating clearly the transition from free-hole to impurity-band conduction. Additional data from [42] for heavy-doped p-GaN were also fitted despite the absence of SIMS measurements of the Mg concentration in the material (not shown here). In the latter case, the Mg concentration was derived from the fitting the temperature-dependent Hall concentration with three parameters, N_A, N_D, and E_A. All the above samples were grown by MOVPE. The data of [43] on p-GaN grown at 750 °C by PAMBE (not shown here) were also included into final consideration, as they represent a low-doping level case, i. e. that with Mg concentration of $5 \cdot 10^{18}\,\mathrm{cm}^{-3}$.

In all the above cases, fitting of the apparent hole concentrations reproduced quite accurately the experimental data. It is important that the accurate fitting is achieved in a wide temperature range, which improves the reliability of the extracted parameters. The only exception was the data obtained at low, 100–150 K, temperatures (Figure 5, F and Figure 6, b). Deviation of the fitting curves from those experimental points could be attributed to the simplified assumption on a temperature independent mobility ratio γ, which might be generally valid in a relatively narrow temperature range only.

The values of the compensating donor concentrations N_D extracted from the processing of TDHM data are plotted in Figure 7, a by symbols as a function of N_A. Approximation of the data (solid line in Figure 7, a) has shown that $N_D \propto N_A^2$. The use of the approximation enables estimating the p-GaN compensation degree $K = N_D/N_A$, which is plotted by dotted line on the right vertical axis of Figure 7, a. One can see K to increase gradually with N_A up to the values of 0.4–0.8 at the Mg concentration ranged from $5 \cdot 10^{20}$ to $1 \cdot 10^{21}\,\mathrm{cm}^{-3}$.

3.2. Ionization energy of Mg acceptors

Figure 7, b demonstrates the well-known trend of decreasing AIE with the concentration of Mg acceptors. Such a trend originates from dependence of the acceptor binding energy on surrounding Mg atoms and can be described by the equation [44]

$$E_A(N_A) = E_A^0 - \alpha f_K N_A^{1/3}, \qquad (10)$$

where E_A^0 is the ionization energy of a single acceptor (or the low-concentration AIE), the constant $\alpha = q^2/4\pi\kappa_0(\kappa_z\kappa_t)^{1/2}$, q is the electron charge, κ_0 is the electric constant, and κ_z and κ_t are the longitudinal and transverse static dielectric constants of GaN, respectively. As it was discussed in [44], f_K is either constant dependent on particular theoretical approach or a function of the compensation degree K. In our study, the function $f_K(K)$ was borrowed from the theoretical analysis by Lien and Shklovskii [45]. At low compensation degree, $f_K(K) \to 1$, being similar to the value proposed by Pearson and Bardin (see references to the respective papers given in [44]). The function approaches its maximum value at $K \approx 0.55$ and becomes negative at $K > 0.93$.

Solid line in Figure 7, b shows the approximation of the extracted data on AIE by Eq. (10) with $E_A^0 = 230$ meV, $\kappa_z = 10.4$, and $\kappa_t = 9.5$ [32] and accounting for the compensation degree dependence on N_A plotted in Figure 7, a. The obtained value of E_A^0 agrees well with the data on low-concentration AIE obtained by PL measurements [1–5]. A specific feature of the approximation curve is its non-monotonic character with the minimum value of 54 meV reached at $N_A = 1.1 \cdot 10^{21}\,\mathrm{cm}^{-3}$. Such a behavior comes from compensation degree impact on AIE via $f_K(K)$ function, which is important for GaN heavily doped with Mg. Unfortunately, the only experimental point corresponding to the sample F in Figure 5 may be regarded as the evidence for such a non-monotonicity. The ever positive AIEs at any concentration of Mg acceptors predicted theoretically means, in particular, that the Mott transition from semiconductor to metal hole conduction can be unlikely achieved.

A comprehensive study of heavily doped GaN:Mg grown by ammonia MBE has been reported in [11]. A substantial decrease in the AIE with the Mg concentration, from 210 down to 60 meV, was also observed on those MBE-grown samples. However, there were two main differences from the results plotted in Figure 7, b. First, the AIE decline in [11] was detected at N_A by an order of magnitude smaller than in the data shown in Figure 7, b. Second, the

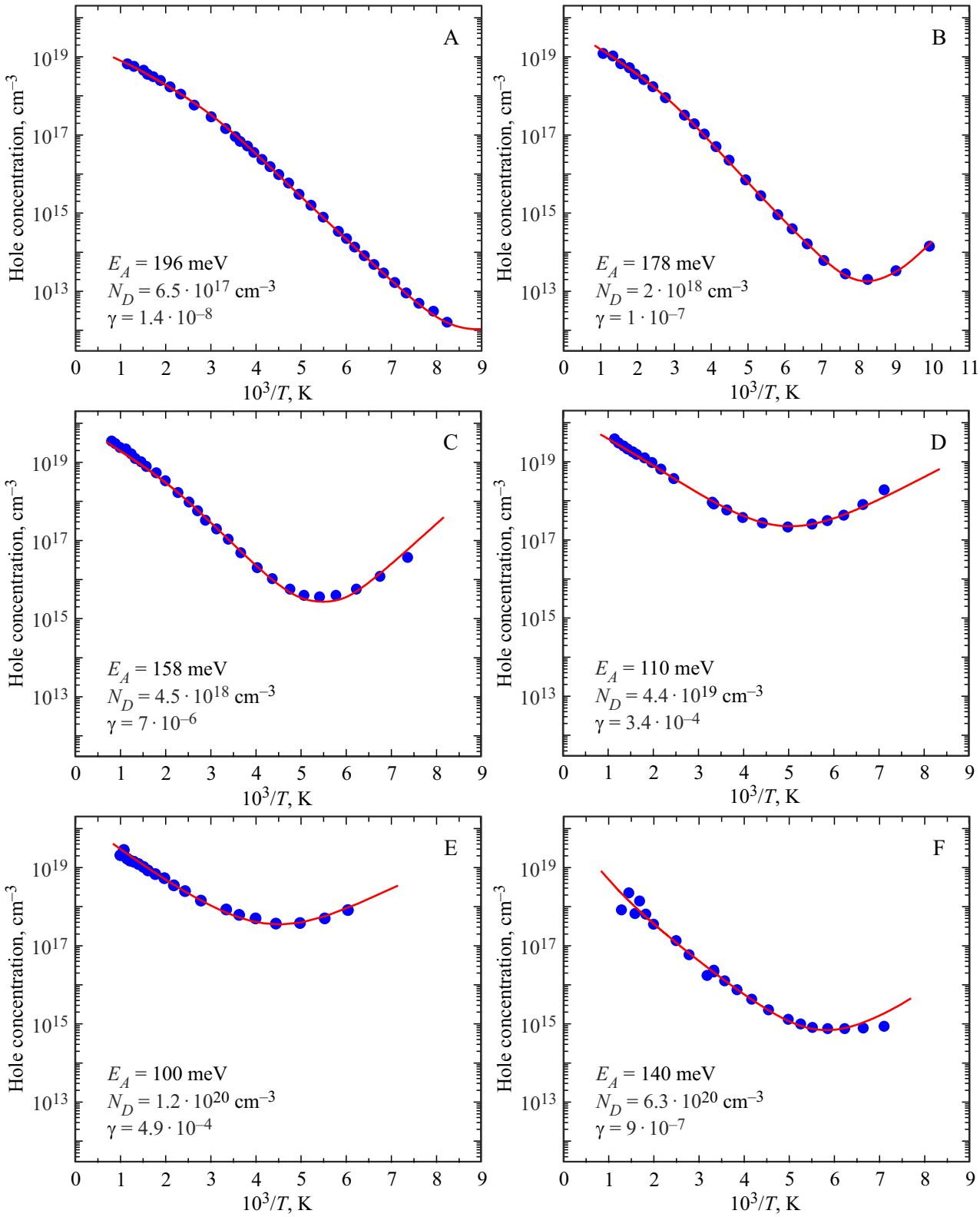


Figure 5. Apparent hole concentration as a function of inverse temperature in heavy-doped *p*-GaN. Circles are data of [17] for the samples with acceptor concentration of (A) $1.6 \cdot 10^{19}$ cm^{-3}, (B) $4 \cdot 10^{19}$ cm^{-3}, (C) $8 \cdot 10^{19}$ cm^{-3}, (D) $2 \cdot 10^{20}$ cm^{-3}, (E) $3 \cdot 10^{20}$ cm^{-3}, and (F) $8 \cdot 10^{20}$ cm^{-3}. Lines are results of fitting with the parameters shown in the legends. Individual graphs are marked by capital letters corresponding to sample designation in Ref. [17].

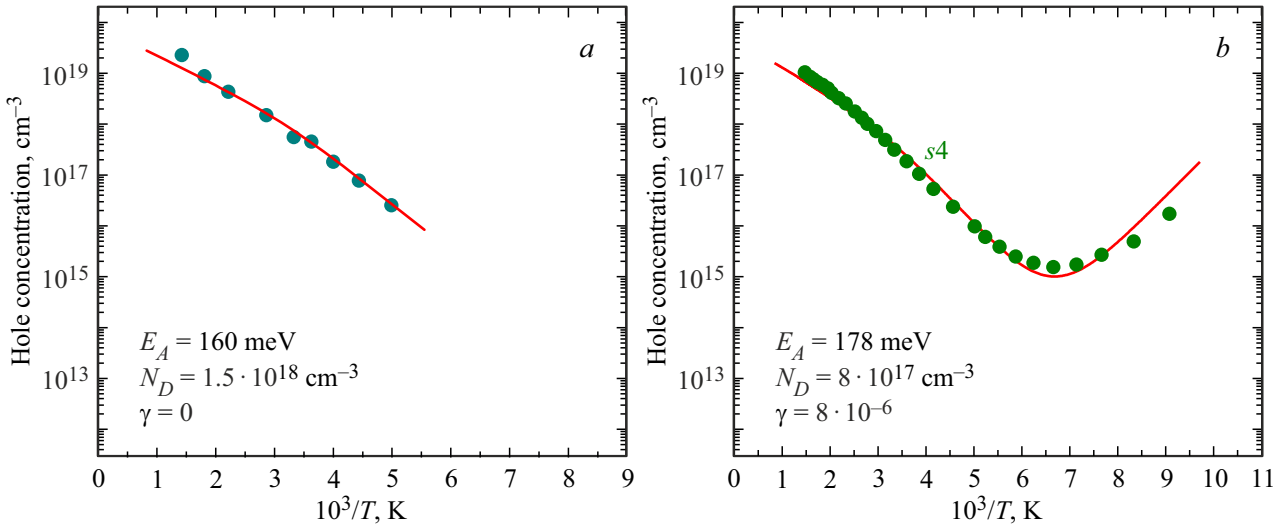


Figure 6. Apparent hole concentration as a function of inverse temperature in p-GaN. Circles are data from (a) Ref. [41] ($N_A = 6.3 \cdot 10^{19}$ cm^{-3}) and (b) Ref. [37] ($N_A = 3 \cdot 10^{19}$ cm^{-3}). Lines are results of fitting with parameters shown in the legends.

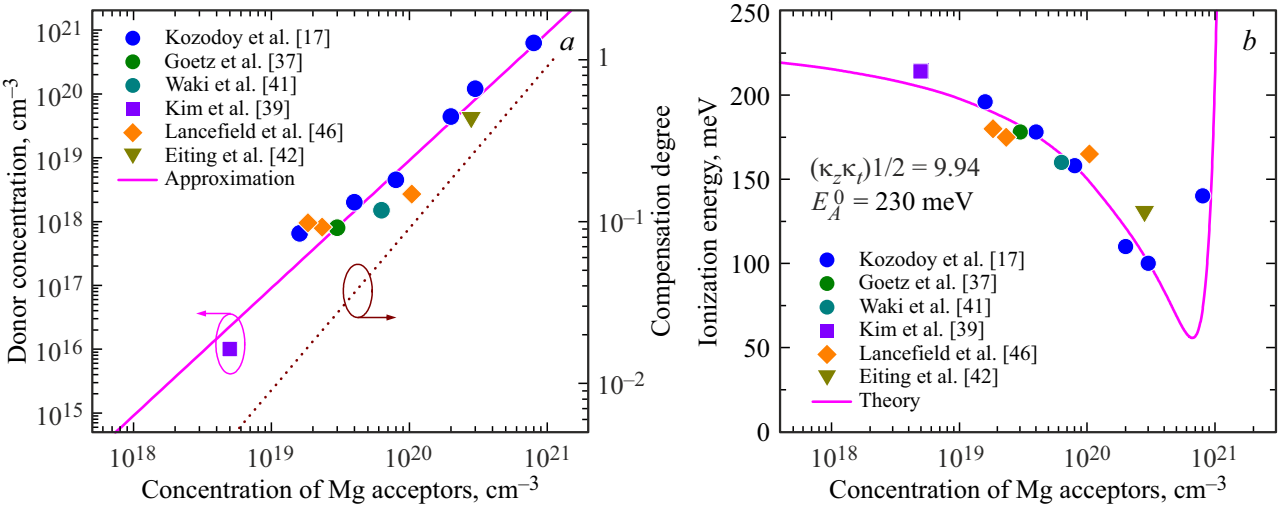


Figure 7. Compensating donor concentration and compensation degree (a) and AIE (b) as a function of Mg acceptor concentration. Symbols are experimental points and lines are theoretical approximations (see text for more detail).

maximum reported values of RT hole concentration were as high, as $6-8 \cdot 10^{18}$ cm^{-3}. In contrast, the maximum hole concentration in the data of [17,40–43,46] selected for this study was $1-2 \cdot 10^{18}$ cm^{-3} (see Figure 8 a). Unfortunately, there was no temperature dependent plots of apparent hole concentrations reported in the paper [11] that would allow judging on whether the temperature range of the Hall measurements was appropriate for accurate extracting the free-hole parameters or not. In particular, the Hall factor $r_H = 1$ was assumed in [11] for the data treatment whereas it might by remarkably lower than unity in the temperature ranges where the impurity-band conduction was noticeable (see Sec. 2.3). Just this factor may be a possible reason for overestimating the RT hole concentration reported in [11]. Besides, the fitting of the apparent hole concentration was made in [11] with a low-k hole isotropic effective mass of $0.8m_0$ (compare with the high-k masses of $1.88-1.89m_0$ used in this study). This factor also might introduce an additional inaccuracy into the parameters extracted in [11].

Along with experimental points on RT hole concentration reported in the papers [17,40–43,46], Figure 8, a displays a theoretical (solid) curve obtained by using Eq. (7) with the parameters E_A and N_D extracted from the fitting the temperature-dependent Hall data. The curve predicts the maximum achievable RT free-hole concentration in GaN:Mg to be of $2 \cdot 10^{18}$ cm^{-3}, being limited by a massive generation of compensating donors at $N_A = 6 \cdot 10^{20}$ cm^{-3}. The dotted line in Figure 8, a shows the corresponding apparent hole concentration p_H calculated by Eq. (8). The concentration p_H starts to deviate remarkably from the free-

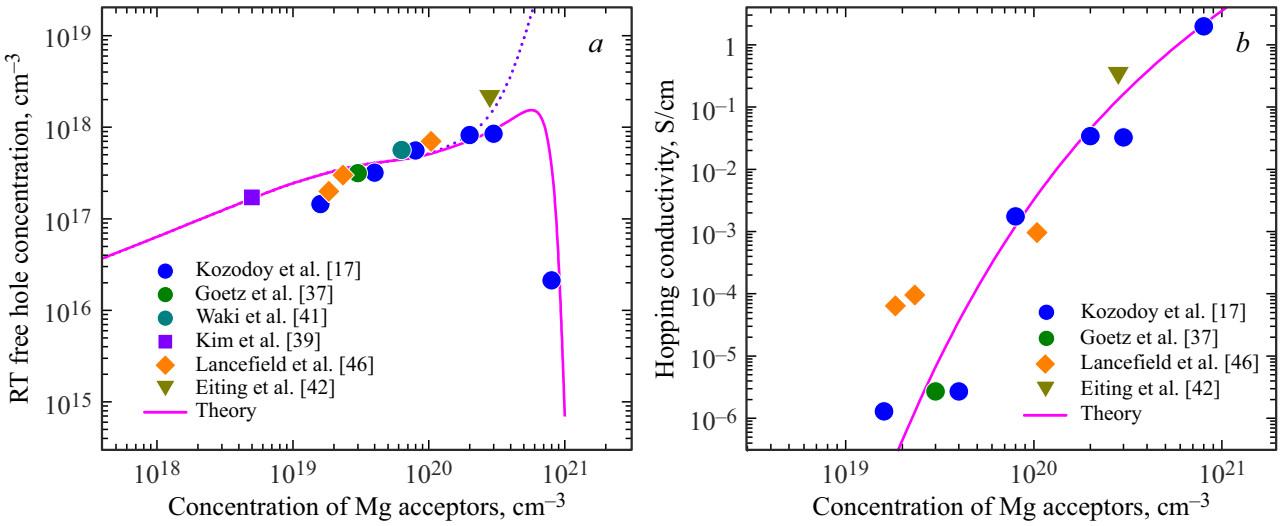


Figure 8. Room-temperature free-hole concentration (a) and hole hopping conductivity (b) as a function of Mg acceptor concentration. Symbols are experimental points, solid lines are theoretical curves. The dotted line indicates the calculated apparent hole concentration p_H (see text for more detail).

hole concentration p towards higher values at N_A exceeding $1-2 \cdot 10^{20}\,\mathrm{cm}^{-3}$. So, at such doping levels p_H cannot be considered as the measure of real free-hole concentration.

3.3. Hopping hole conduction in GaN:Mg

Treatment of the Hall data by the two-carrier model enables assessment of the role of hole conduction via impurity band. In accordance with the consideration made in Sec. 2.3, the impurity-band electrical conductivity of holes is $\sigma_h = q\mu_h N_A^0$ where N_A^0 is the concentration of neutral acceptors or, which is the same, of the holes bound with the acceptors. In order to estimate σ_h, it is necessary to consider the temperature $T_{\min}$ corresponding to the minimum of apparent hole concentration p_H in every temperature-dependent curve shown, for instance, in Figure 5 and Figure 6. At this temperature, electrical conductivities of free holes σ_p and bound holes σ_h are nearly equal to each other. Therefore, the impurity-band electrical conductivity can be estimated by the relationship $\sigma_h \cong \frac{1}{2} q\mu_{\min} p_{\min}$ where $p_{\min} \equiv p_H(T_{\min})$ and $\mu_{\min} \equiv \mu_H(T_{\min})$ are the apparent hole concentration and mobility at the temperature $T_{\min}$ respectively.

Figure 8, b plots by symbols the values of the impurity-band electrical conductivity estimated in such a way from the data of [17,40–43,46] versus Mg concentration. The experimental points can be well approximated by the theoretical dependence

$$\sigma_h(N_A) = \sigma_{03} \exp(-\beta / a_B N_A^{1/3}), \qquad (11)$$

where $\sigma_{03} = 100\,\mathrm{Sm/cm}$, $a_B = (2m_{hh}E_A)^{1/2}/\hbar$ is the Bohr radius of the acceptor wave function corresponding to the concentration-dependent ionization energy E_A, $m_{hh} = (m_{hh}^t)^{2/3}(m_{hh}^z)^{1/3}$ is the mean effective mass of heavy holes, $\hbar$ is the Plank constant, and $\beta = 1.73$ is the numerical coefficient derived by Shklovskii and Efros on the basis of percolation theory [40]. Good agreement between the theory and experiments, including the particular value of the β-coefficient, is the evidence for hopping mechanism of impurity-band hole conduction in GaN:Mg.

Analysis of the $p_H(T)$ dependencies shown in Figures 5, 6 has shown that the slopes of the curves to the right and to the left of the point $1000/T_{\min}$ are nearly equal to each other in most cases. This has been earlier explained in the book [40] by the fact that temperature dependence of the conductivity σ_{03} is largely determined by AIE, similarly to the conductivity of free holes. It is also interesting that the hopping conduction of holes in GaN is a relatively high-temperature phenomenon, in contrast to most cases of other semiconductors discussed in [40]. Indeed, the temperature $T_{\min}$, at which the impurity-band (hopping) conduction of holes becomes noticeable, rises from about 100 K at $N_A = 1.5 \cdot 10^{19}\,\mathrm{cm}^{-3}$ to 225–250 K at $N_A = 3 \cdot 10^{20}\,\mathrm{cm}^{-3}$. Therefore, GaN:Mg represents a quite suitable object for investigations into hopping conduction, just thanks to a rather high AIE.

3.4. Compensation of Mg acceptors in GaN

Solid line in Figure 7, a, satisfying the relationship $N_D = N_A^2/N_r$ with $N_r = 1.1 \cdot 10^{21}\,\mathrm{cm}^{-3}$, represents the approximation of the experimental points corresponding to concentrations of the compensating donors extracted from the TDHM data. The above relationship demonstrates a distinct correlation between the concentration of Mg acceptors N_A and donor concentration N_D.

Using first-principles DFT calculations, Miceli and Pasquarello suggested formation of Mg interstitials to

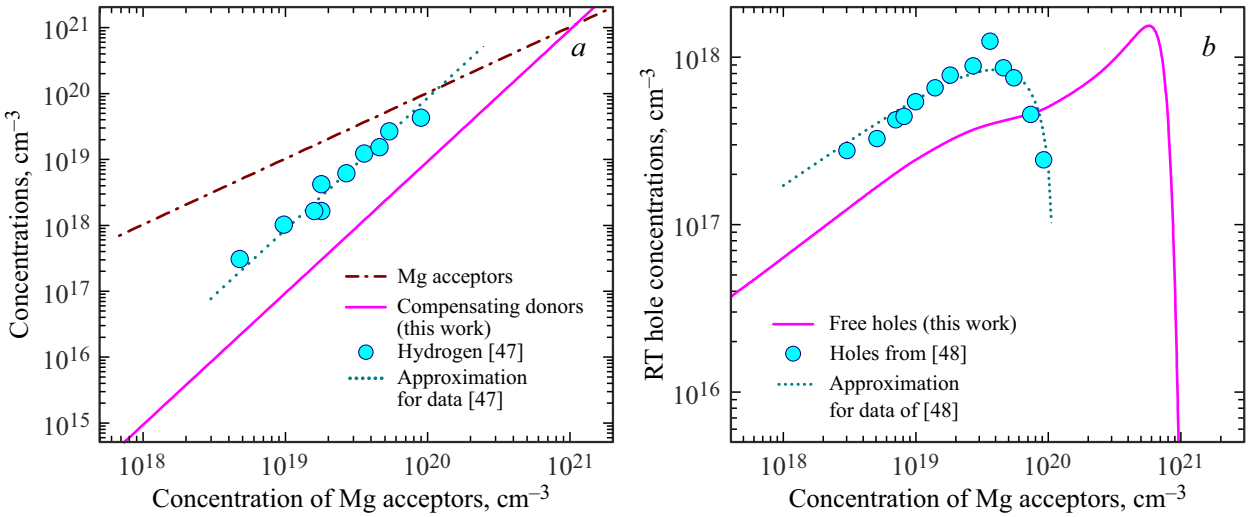


Figure 9. Comparison of residual hydrogen concentration in GaN:Mg reported in [47] with the concentration of compensating donors derived in this work (*a*) and comparison of RT hole concentration from [47] and from this work (*b*) as functions of Mg acceptor concentration. Symbols are experimental points from [47], solid lines are results of our study. The dotted lines are approximations of the data from [47] whereas dot-dashed line indicates the concentration of Mg acceptors given for reference.

be the principal mechanism of the Mg acceptor self-compensation [24]. They have rejected an equilibrium model of the defects as that incapable of explaining both qualitatively and quantitatively the data of [15] on self-compensation of Mg acceptors. An alternative non-equilibrium model also suggested in [24] was fitted to particular experimental points of Ref. [15], thus providing a reasonable agreement with the RT hole concentrations near the self-compensation threshold. However, the later model predicted the concentration of compensating donors $N_D \propto N_A^8$, which differed dramatically from the experimental trend found in this work by processing the data of [17,40–43,46].

In order to shed light on the nature of the compensating donors, let us consider the recent data of [47]. In that study, authors examined by Hall measurements a series of MOVPE-grown GaN samples heavily doped with Mg after careful post-growth annealing of the samples. Symbols in Figure 9, *a* show the data on residual concentration of hydrogen atoms (measured in [47] by SIMS) still existing in the GaN bulk after annealing aimed at the hydrogen releasing from the crystal. The dotted line approximating the data goes parallel to the solid line borrowed from Figure 7, *a* and represented the concentration of the compensating donors in GaN:Mg samples from Refs. [17,40–43,46]. The same slopes of both lines mean that the residual hydrogen concentration measured in [47] is proportional to N_A^2 similarly to the concentration of compensating donors derived in this work. Therefore, it is reasonable to attribute the compensation donors to some kind of defects containing both Mg and H atoms and formed in GaN:Mg either during growth or/and during annealing stage.

Figure 9, *a* shows also that the concentration of residual hydrogen (compensating donor) measured in [47] turns out by an order of magnitude higher than N_D found in this study. Correspondingly, the hydrogen concentration (approximated by dotted line in Figure 9, *a*) is expected to approach the Mg acceptor concentration (dot-dashed line in Figure 9, *a*) at N_A by about an order of magnitude lower than in the cases considered here (see the intersection of solid lines with the dot-dashed line in Figure 9, *a*). When N_D becomes close to N_A, the self-compensation of the Mg acceptors starts to occur, resulting in a dramatic drop of the RT hole concentration. The latter is clearly seen in Figure 9b where the maximum of the RT hole concentration $p_{\max}$ reported in [47] is observed at $N_{\max}$ by an order of magnitude lower than in the GaM:Mg samples from [17,40–43,46]. A similar situation takes place with the data of [11] and [15]. Such a big difference between $p_{\max}$ and $N_{\max}$ reported in [11,15,47] and those obtained in [17,40–43,46] is the evidence for essential dependence of residual hydrogen (compensation donor) concentration on particular growth and/or annealing conditions. The latter may also explain the large scatter in $p_{\max}$ and $N_{\max}$ values reported in previous publications (see also Table 1).

There are a few point defects regarded in literature that would contain both Mg and H atoms. The frequently discussed complex of substitutional Mg with interstitial H, $Mg_{Ga}-H_I$, can be withdrawn from the list of candidates for compensating donors since it is electrically neutral practically in the whole range of the Fermi level variation inside the bandgap [9,48] and, therefore, cannot compensate Mg acceptors. By the same reason, the triple complex $Mg_{Ga}-Mg_{Ga}-H_I$ investigated in [48] can be withdrawn too. The interstitial H_I by itself, being a single donor in *p*-type GaN, could be potentially regarded as the defect initiating self-compensation of Mg acceptors. However, it is very mobile and can be easily released from the crystal

during thermal annealing. Besides, correlation of its intrinsic concentration in GaN with Mg concentration is not visible. Nevertheless, first-principle calculations carried out in [48] predict the existence of one more complex, $Mg_{Ga}-H_N$, being a single donor at any Fermi level position and having the formation energy a little bit greater than that of H_I. As it is a complex defect, its mobility is expected to be low and, therefore, the complex seems to be resistant to thermal annealing. Therefore, it may play the role of compensating donors in heavily doped GaN:Mg.

4. Conclusions

In this paper, available in literature well-performed TDHMs were reconsidered in order to get a deeper insight into *p*-type doping GaN with Mg in a wide concentration range. To be accurate, processing of the Hall data should employ carefully defined materials parameters, like temperature-dependent degeneracy factor of holes and their effective masses, and account for contribution of all three valence bands to the effective density of hole states. Experimental determination of the AIE dependence on the Mg acceptor concentration in GaN requires to use a wide range of temperature variation, including the margin well above RT. Extension of the temperature range down to below $220-250\,K$ enables monitoring of hopping hole conduction occurring in GaN at high doping levels. In this case, processing of the Hall data should account for both free-hole and impurity-band hole conduction via two-carrier model. If not, processing of the Hall measurements carried out below RT may overestimate the extracted hole concentrations, because of indistinguishable holes occupying both valence and impurity bands.

Ionization energy of Mg acceptors as a function of their concentration N_A is extracted from the Hall data, accounting for their partial compensation with donor defects. The concentration of compensating donors N_D is found to be proportional to the square of N_A. In the considered samples, the compensation ratio N_D/N_A rose up to the value of $\sim 79\,\%$ at maximum concentration $N_A = 8 \cdot 10^{20}\,cm^{-3}$, resulting in non-monotonous AIE dependence on N_A. A similar non-monotonicity caused by compensation has been earlier predicted theoretically by Lien and Shklovskii [45].

In all the considered samples with $N_A > 5 \cdot 10^{19}\,cm^{-3}$, the hole conduction via impurity band was observed at relatively low temperatures, leading to inversion of the slope in the dependence of apparent hole concentration p_H on inverse temperature $(1/T)$. The inversion occurred at a certain temperature T_{min} risen from $100\,K$ at $N_A = 1.5 \cdot 10^{19}\,cm^{-3}$ to $\sim 225-250\,K$ at $N_A = 3 \cdot 10^{20}\,cm^{-3}$, demonstrating the impurity-band conduction to be a rather high-temperature process in GaN. The dependence of the impurity-band electrical conductivity on acceptor concentration N_A extracted from the Hall data is found to be in excellent agreement with the numerical calculations by Shklovsky and Efros based on the percolation theory [40]. The agreement is the evidence for hopping mechanism of hole conduction in the impurity band.

Similar dependences of N_D found in this study and residual hydrogen concentration from [47] on N_A enables suggestion of a new mechanism of Mg acceptor self-compensation, involving generation of $Mg_{Ga}-H_N$ complex defects either during growth of GaN:Mg or/and during its post-growth annealing. Since the complexes are expected to have a mobility much lower than that of interstitial hydrogen, they should be resistant to thermal annealing, eventually determining the compensation degree of Mg acceptors.

The processing of the selected Hall data has shown the maximum RT hole concentration to approach $1-2 \cdot 10^{18}\,cm^{-3}$ at $N_A = 3-5 \cdot 10^{20}\,cm^{-3}$. The both values lie well above the similar parameters ($p_{max} = 6 \cdot 10^{17}\,cm^{-3}$ and $N_{max} = 2 \cdot 10^{19}\,cm^{-3}$) reported, for example, in [15]. Such a big experimental scatter in the values of p_{max} and N_{max} is attributed to different conditions of GaN:Mg growth and/or post-growth annealing, eventually resulting in different residual concentration of the compensating $Mg_{Ga}-H_N$ defects. On the other hand, the results reported in [17,40–43,46] have demonstrated the existence of optimal growth/annealing recipes leading to minimization of the residual concentration of compensating defects. A deeper understanding of the impact of growth/annealing conditions on self-compensation of Mg acceptors is the subject of future studies, as well as their extension to AlGaN alloys serving as the basis for development of ultra-violet light sources.

Conflict of interest

The authors declare no conflicts of interest.

References

[1] S. Fischer, C. Wetzel, E.E. Haller, and B.K. Meyer, *On p-type doping in GaN — acceptor binding energies*, Appl. Phys. Lett. **67**, 1298 (1995).

[2] Wook Kim, A.E. Botchkarev, A. Salvador, G. Popovici, H. Tang, and H. Morkoç, *On the incorporation of Mg and the role of oxygen, silicon, and hydrogen in GaN prepared by reactive molecular beam epitaxy*, J. Appl. Phys. **82**, 219 (1997).

[3] S. Strauf, P. Michler, J. Gutowski, U. Birkle, M. Fehrer, S. Einfeldt, and D. Hommel, *Optical Spectroscopy of Mg- and C-Related Donor and Acceptor Levels in GaN Grown by MBE*, Phys. Stat. Solidi B **216**, 557 (1999).

[4] S. Strauf, S.M. Ulrich, P. Michler, J. Gutowski, T. Böttcher, S. Figge, S. Einfeldt, and D. Hommel, *Analysis of Time-Resolved Donor-Acceptor-Pair Recombination in MBE and MOVPE Grown GaN:Mg*, Phys. Stat. Solidi B **228**, 379 (2001).

[5] M.A. Reshchikov, P. Ghimire, and D.O. Demchenko, *Magnesium acceptor in gallium nitride. I. Photoluminescence from Mg-doped GaN*, Phys. Rev. B **97**, 205204 (2018).

[6] F. Mireles and S.E. Ulloa, *Acceptor binding energies in GaN and AlN*, Phys. Rev. B **5**8, 3879 (1998).
[7] H. Wang and A.-B. Chen, *Calculations of acceptor ionization energies in GaN*, Phys. Rev. B **63**, 125212 (2001).
[8] V. Fiorentini, F. Bernardini, A. Bosin, and D. Vanderbilt, *Ab initio shallow acceptor levels in gallium nitride*, arXiv:cond-mat/9610045v1 [cond-mat.mtrl-sci]
[9] J.L. Lyons, A. Janotti, and C.G. Van de Walle, *Shallow versus Deep Nature of Mg Acceptors in Nitride Semiconductors*, Phys. Rev. Lett. **108**, 156403 (2012).
[10] M.A. Reshchikov, D.O. Demchenko, J.D. McNamara, S. Fernández-Garrido, and R. Calarco, *Green luminescence in Mg-doped GaN*, Phys. Rev. B **90**, 035207 (2014).
[11] S. Brochen, J. Brault, S. Chenot, A. Dussaigne, M. Leroux, and B. Damilano, *Dependence of the Mg-related acceptor ionization energy with the acceptor concentration in p-type GaN layers grown by molecular beam epitaxy*, Appl. Phys. Lett. **103**, 032102 (2013).
[12] M. Chlipala, H. Turski, M. Siekacz, K. Pieniak, K. Nowakowski-Szkudlarek, T. Suski, and C. Skierbiszewski, *Nitride light-emitting diodes for cryogenic temperatures*, Optics Express **28**, 30299 (2020).
[13] Changeun Park, Jaehyeok Park, Sangjin Min, Jong-In Shim, and Dong-Soo Shin, *Origin of the High Forward Voltage and Low Voltage Efficiency of GaN-Based Light-Emitting Diodes at Cryogenic Temperatures*, ACS Photonics **11**, 464 (2024).
[14] Hao-Jen Chang, Ke-Hsi Chiang, Yu-Ming Jao, Yuan-Chao Wang, Min-Hsiung Shih, Haj-Chung Kuo, Jian-Jang, Huang, and Chien-Chung Lin, *Photonic properties of InGaN-based micro LEDs in the cryogenic temperature regime*, Optics Express **32**, 44898 (2024).
[15] U. Kaufmann, P. Schlotter, H. Obloh, K. Köhler, and M. Maier, *Hole conductivity and compensation in epitaxial GaN:Mg layers*, Phys. Rev. B **62**, 10867 (2000).
[16] I.P. Smorchkova, E. Haus, B. Heying, P. Kozodoy, P. Fini, J.P. Ibbetson, S. Keller, S.P. DenBaars, J.S. Speck, and U.K. Mishra, *Mg doping of GaN layers grown by plasma-assisted molecular-beam epitaxy*, Appl. Phys. Lett. **76**, 718 (2000).
[17] P. Kozodoy, Huili Xing, S.P. DenBaars, U.K. Mishra, A. Saxler, R. Perrin, S. Elhamri, and W.C. Mitchel, *Heavy doping effects in Mg-doped GaN*, J. Appl. Phys. **87**, 1832 (2000).
[18] L.T. Romano, M. Kneissl, J.E. Northrup, C.G. Van de Walle and D.W. Treat, *Influence of microstructure on the carrier concentration of Mg-doped GaN films*, Appl. Phys. Lett. **79**, 2734 (2001).
[19] J.F. Kaeding, H. Asamizu, H. Sato, M. Iza, T.E. Mates, S.P. DenBaars, J.S. Speck, and S. Nakamura, *Realization of high hole concentrations in Mg doped semipolar* $(10\bar{1}\bar{1})$ *GaN*, Appl. Phys. Lett. **89**, 202104 (2006).
[20] H.R. Qi, S. Zhang, S.T. Liu, F. Liang, L.K. Yi, J.L. Huang, M. Zhou, Z.W. He, D.G. Zhao, and D.S. Jiang, *The self-compensation effect of heavily Mg doped p-GaN films studied by SIMS and photoluminescence*, Superlattices and Microstructures **133**, 106177 (2019).
[21] Jin-Ji Dai, Thi Thu Mai, Ssu-Kuan Wu, Jing-Rong Peng, Cheng-Wei Liu, Hua-Chiang Wen, Wu-Ching Chou, Han-Chieh Ho and Wei-Fan Wang, *High Hole Concentration and Diffusion Suppression of Heavily Mg-Doped p-GaN for Application in Enhanced-Mode GaN HEMT*, Nanomaterials **11**, 1766 (2021).
[22] Siyi Huang, M. Ikeda, Feng Zhang, Minglong Zhang, Jianjun Zhu, Shuming Zhang, and Jianping Liu, *Achievable hole concentration at room temperature as a function of Mg concentration for MOCVD-grown p-GaN after sufficient annealing*, J. Semiconductors **45**, 082501 (2024).
[23] A. Naito, K. Ueno, A. Kobayashi, and H. Fujioka, *Hole Conduction Mechanism in In–Mg-Codoped GaN Prepared via Pulsed Sputtering Deposition*, Phys. Status Solidi A **221**, 230806 (2024).
[24] G. Miceli and A. Pasquarello, *Self-compensation due to point defects in Mg-doped GaN*, Phys. Rev. B **93**, 165207 (2016).
[25] F. Shahedipour and B.W. Wessels, *Investigation of the formation of the 2.8 eV luminescence band in p-type GaN:Mg*, Appl. Phys. Lett. **76**, 3011 (2000).
[26] A. Uedono, S. Takashima, M. Edo, K. Ueno, H. Matsuyama, H. Kudo, H. Naramoto, and S. Ishibashi, *Vacancy-type defects and their annealing behaviors in Mg-implanted GaN studied by a monoenergetic positron beam*, Phys. Status Solidi B **252**, 2794 (2015).
[27] G.L. Bir and G.E. Pikus, *Symmetry and strain-induced effects in semiconductors*, (John Wiley & Sons, NY, 1974).
[28] S.L. Chuang and C.S. Chang, $\mathbf{k}\cdot\mathbf{p}$ *method for strained wurtzite semiconductors*, Phys. Rev. B **54**, 2491 (1996).
[29] A.V. Malyshev, I.A. Merkulov and A.V. Rodina, *Ground-state characteristics of an acceptor center in wide-gap semiconductors with a weak spin-orbit coupling*, Phys. Solid State **40**, 917 (1998).
[30] A.A. Yamaguchi, Y. Mochizuki, H. Sunakawa, and A. Usui, *Determination of valence band splitting parameters in GaN*, J. Appl. Phys. **83**, 4542 (1998).
[31] P. Rinke, M. Winkelnkemper, A. Qteish, D. Bimberg, J. Neugebauer, and M. Scheffler, *Consistent set of band parameters for the group-III nitrides AlN, GaN, and InN*, Phys. Rev. B **77**, 075202 (2008).
[32] H. Morkoç, *Handbook of Nitride Semiconductors and Devices*, (WILEY-VCH Verlag GmbH & Co. KGaA, Weinheim, 2008).
[33] Y. Nakano and T. Jimbo, *Electrical Properties of Acceptor Levels in Mg-Doped GaN*, phys. stat. sol. (c) **0**, 438 (2002).
[34] J.W. Huang, T.F. Kuech, H. Lu and I. Bhat, *Electrical characterization of Mg-doped GaN grown by metalorganic vapor phase epitaxy*, Appl. Phys. Lett. **68**, 2392 (1996).
[35] D. Seghier and H.P. Gislason, *Electrical characterization of Mg-related energy levels and the compensation mechanism in GaN:Mg*, J. Appl. Phys. **88**, 6483 (2000).
[36] J.W. Huang, T.F. Kuech, Hongqiang Lu, and I. Bhat, *Electrical characterization of Mg-doped GaN grown by metalorganic vapor phase epitaxy*, Appl. Phys. Lett. **68**, 2392 (1996).
[37] W. Götz, R.S. Kern, C.H. Chen, H. Liu, D.A. Steigerwald, and R.M. Fletcher, *Hall-effect characterization of III–V nitride semiconductors for high efficiency light emitting diodes*, Mat. Sci. Engineering B **59**, 211 (1999).
[38] H. Nakayama, P. Hacke, M.R.H. Khan, T. Detchprohm, K. Hiramatsu, and N. Sawaki, *Electrical Transport Properties of p-GaN*, Jpn. J. Appl. Phys. **35**, L282 (1996).
[39] D.J. Kim, D.Y. Ryu, N.A. Bojarczuk, J. Karasinski, S. Guha, S.H. Lee, and J.H. Lee, *Thermal activation energies of Mg in GaN:Mg measured by the Hall effect and admittance spectroscopy*, J. Appl. Phys. **88**, 2564 (2000).
[40] B.I. Shklovsky and A.L. Efros, *Electronic Properties of Doped Semiconductors*, (Springer, Berlin, 1984).

[41] I. Waki, H. Fujioka, M. Oshima, H. Miki, and A. Fukizawa, *Activation of Mg-doped GaN by Thermal Annealing in Oxidizing Atmospheres*, Proc. Int. Conf. Nitride Semiconductors, IPAP Conf. Ser. **1**, 728 (2000).
[42] C.J. Eiting, P.A. Grutdowski and R.D. Dupuis, *Growth of low resistivity p-type GaN by metal organic chemical vapour deposition*, Electron. Lett. **33**, 1987 (1997).
[43] Wook Kim, A. Salvador, A.E. Botchkarev, O. Aktas, S.N. Mohammad, and H. Morkoc, *Mg-doped p-type GaN grown by reactive molecular beam epitaxy*, Appl. Phys. Lett. **69**, 559 (1996).
[44] B. Pődör, *Thermal ionization energy of Mg acceptors in GaN: Effects of doping level and compensation*, Proc. SPIE **4412**, 299 (2000).
[45] Nguyen Van Lien and B.I. Shklovskii, *Percolation level of a highly compensated semiconductor*, Soviet Physics. Semiconductors. **13**, 1025 (1979).
[46] D. Lancefield and H. Eshghi, *Temperature-dependent hole transport in GaN*, J. Phys.: Condens. Matter **13**, 8939 (2001).
[47] Siyi Huang, Masao Ikeda, Feng Zhang, Minglong Zhang, Jianjun Zhu, Shuming Zhang, and Jianping Liu, *Achievable hole concentration at room temperature as a function of Mg concentration for MOCVD-grown p-GaN after sufficient annealing*, J. Semicond. **45**, 082501 (2024).
[48] Menglin Huang, He Li, and Shiyou Chen, *Triple-Site Dopant–Defect Complexes in Mg−H-Codoped GaN: First-Principles Identification*, Phys. Status Solidi A **218**, 2000723 (2021).